Molecular Dynamics Simulations of NAD^+ in Solution

Paul E. Smith*,† and John J. Tanner*,‡

Contribution from the Department of Biochemistry, Kansas State University, Manhattan, Kansas 66506-3702, and Department of Chemistry, University of Missouri-Columbia, Columbia, Missouri 65211

Received May 14, 1999

Abstract: Molecular dynamics simulations in explicit solvent have been performed to investigate the conformational preferences of NAD^+ in solution. Two simulations, started from different initial conformations, generated similar results. Transitions between different folded forms of the molecule were observed. The simulations predict that the predominant form of NAD^+ in solution is a folded conformation characterized by a nicotinamide−adenine inter-ring distance of 0.52 nm, an angle of 148° between the aromatic ring planes, parallel glycosyl bond vectors, and the nicotinamide B side facing the adenine ring. Analysis of the NAD^+ conformations generated during the simulations suggests that folded conformations are favored over extended ones due to the reduction in solvent-accessible surface area, while differences between folded conformations correlate with changes in the solvation properties of the nicotinamide group. The simulation results are consistent with NMR relaxation data, and they argue against previous proposals that intimate, parallel ring stacking is the hallmark of the folded conformation of NAD^+.

Introduction

Nicotinamide adenine dinucleotide (NAD) is a ubiquitous coenzyme and substrate. NAD is a major unit of currency in biological redox chemistry. Over 100 NAD dependent dehydrogenases are known, such as those that catalyze the oxidation of glyceraldehyde-3-phosphate, ethanol, lactate, and malate. In these enzymes, the oxidized form of NAD (NAD^+) is reduced by accepting a hydride ion at the nicotinamide C4 position. The reduced form of NAD (NADH) provides the reducing electrons for mitochondrial ATP production. NADH is also a substrate for NADH oxidase/flavin reductase enzymes,[1−5] which produce reduced flavin for the bacterial luciferase light emitting reaction, among other roles.[6] In addition to its redox function, NAD^+ is a labile substrate for ADP ribosylating enzymes, which cleave the nicotinamide glycosyl bond.[7,8] NAD is of practical importance because analogues of this molecule are potentially useful as anticancer[9−11] antibacterial,[12] and antitrypanosomal agents.[13−16]

Knowledge of the three-dimensional structures and dynamics of enzyme-bound and free forms of NAD is important for understanding its many biochemical roles and for designing analogues for therapeutic applications. While much is known about the structures of enzyme-bound NAD, the solution structure of NAD and the dynamics of NAD−enzyme encounters are less well characterized.

NAD^+ bound to enzymes typically adopts extended conformations in which the distance between the nicotinamide C2 and adenine C6 is 0.8−1.8 nm.[17] Perhaps the most recognizable example of an extended NAD^+ is that bound to a pair of mononucleotide-binding (or Rossmann fold) domains, in which each half of the coenzyme binds to a pair of $\beta-\alpha-\beta$ motifs.[18] A crystal structure of the Li^+ salt of NAD^+ in the absence of protein has been determined, and that structure also reveals an extended molecule with a C2−C6 distance of 1.2 nm.[19,20]

* Corresponding authors J.J.T. and P.E.S., respectively: (tel.): 573-884-1280 (J.J.T. only); (fax) 573-882-2754, 785-532-7278; (e-mail) tannerjj@missouri.edu, pesmith@ksu.edu.

† Kansas State University.

‡ University of Missouri-Columbia.

(1) Koike, H.; Sasaki, H.; Kobori, T.; Zenno, S.; Saigo, K.; Murphy, M. E.; Adman, E. T.; Tanokura, M. *J. Mol. Biol.* **1998**, *280*, 259−73.

(2) Zenno, S.; Koike, H.; Tanokura, M.; Saigo, K. *J. Bacteriol.* **1996**, *178*, 4731−3.

(3) Zenno, S.; Koike, H.; Kumar, A. N.; Jayaraman, R.; Tanokura, M.; Saigo, K. *J. Bacteriol.* **1996**, *178*, 4508−14.

(4) Lei, B.; Liu, M.; Huang, S.; Tu, S.-C. *J. Bacteriol.* **1994**, *176*, 3552−8.

(5) Lei, B.; Tu, S.-C. *Characterization of the Vibrio harveyi FMN: NADPH oxidoreductase expressed in Escherichia coli*; Lei, B., Tu, S.-C., Eds.; Walter de Gruyter: Berlin, 1994; pp 847−850.

(6) Tu, S.-C.; Mager, H. I. X. *Photochem. Photobiol.* **1995**, *62*, 615−624.

(7) Jacobson, M. K.; Jacobson, E. L. *ADP-ribose transfer reactions. Mechanisms and biological significance*; Springer-Verlag: New York, 1989.

(8) Althaus, F. R.; Richter, C. *ADP-ribosylation of proteins*; Springer-Verlag: Berlin, 1987; Vol. 37.

(9) Nagai, M.; Natsumeda, Y.; Konno, Y.; Hoffman, R.; Irino, S.; Weber, G. *Cancer Res.* **1991**, *51*, 3886−90.

(10) Franchetti, P.; Cappellacci, L.; Perlini, P.; Jayaram, H. N.; Butler, A.; Schneider, B. P.; Collart, F. R.; Huberman, E.; Grifantini, M. *J. Med. Chem.* **1998**, *41*, 1702−7.

(11) Konno, Y.; Natsumeda, Y.; Nagai, M.; Yamaji, Y.; Ohno, S.; Suzuki, K.; Weber, G. *J. Biol. Chem.* **1991**, *266*, 506−9.

(12) Zhang, R.-g.; Evans, G.; Rotella, F. J.; Westbrook, E. M.; Beno, D.; Huberman, E.; Joachimiak, A.; Collart, F. R. *Biochemistry* **1999**, *38*, 4691−700.

(13) Aronov, A. M.; Verlinde, C. L.; Hol, W. G.; Gelb, M. H. *J. Med. Chem.* **1998**, *41*, 4790−9.

(14) Van Calenbergh, S.; Verlinde, C. L., Soenens, J.; De Bruyn, A.; Callens, M.; Blaton, N. M.; Peeters, O. M.; Rozenski, J.; Hol, W. G.; Herdewijn, P. *J. Med. Chem.* **1995**, *38*, 3838−49.

(15) Verlinde, C. L.; Merritt, E. A.; Van den Akker, F.; Kim, H.; Feil, I.; Delboni, L. F.; Mande, S. C.; Sarfaty, S.; Petra, P. H.; Hol, W. G. *Protein Sci.* **1994**, *3*, 1670−86.

(16) Verlinde, C. L.; Callens, M.; Van Calenbergh, S.; Van Aerschot, A.; Herdewijn, P.; Hannaert, V.; Michels, P. A.; Opperdoes, F. R.; Hol, W. G. *J. Med. Chem.* **1994**, *37*, 3605−13.

(17) Bell, C. E.; Yeates, T. O.; Eisenberg, D. *Protein Sci.* **1997**, *6*, 2084−96.

(18) Brändén, C.; Tooze, J. *Introduction to protein structure*; Garland Publishing, Inc.: New York, 1991.

(19) Reddy, B. S.; Saenger, W.; Mühlegger, K.; Weimann, G. *J. Am. Chem. Soc.* **1981**, *103*, 907−14.

(20) Saenger, W.; Reddy, B. S.; Mühlegger, K.; Weimann, G. *Nature (London)* **1977**, *267*, 225−9.

10.1021/ja991624b CCC: $18.00
Published on Web 09/03/1999

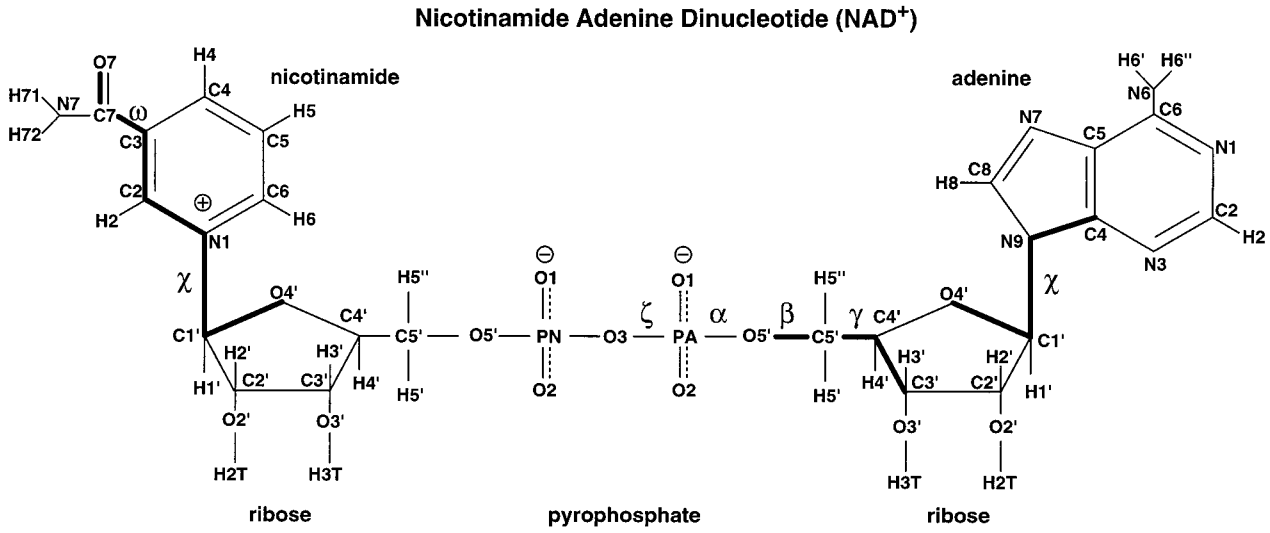

Figure 1. Chemical structure and nomenclature of NAD^+. Dihedral angles are noted by Greek letters. The thick bonds indicate the dihedral angle definitions for γ, χ, and ω.

In contrast, fluorescence spectroscopy,[21,22] circular dichroism,[23] and NMR[24−33] studies of NAD^+ in solution suggest a more compact structure. While a consensus atomic-level model has not emerged from these data, and the interpretation of some of the NMR data has been questioned,[34] NAD^+ in solution is thought to be a mixture of folded and unfolded forms with the aromatic rings in close proximity in the folded form. There is disagreement, however, over the nature and extent of the interaction between the aromatic rings in the folded form. Some groups have proposed that parallel-ring stacking with an inter-ring distance of less than 0.39 nm is the hallmark of the folded form of NAD^+,[23,25,27,29] while others have proposed a "less restrictive"[32,33] description of the folded form in which the inter-ring distance is greater than 0.45 nm and the aromatic rings are not perfectly stacked in parallel.[24]

The idea that NAD^+ is folded in solution contrasts sharply with the crystal structures of enzyme-bound NAD^+ and implies that the dinucleotide must unfold to be catalytically useful. Little is known about the dynamics of this process, nor is it known how, or even if, the enzyme assists in the unfolding of the dinucleotide during catalysis.

Table 1. Summary of MD Simulations

	MD 1	MD 2
total simulation time	5 ns	2.5 ns
total no. of atoms	2671	2671
no. of NAD atoms	70	70
no. of water molecules	867	867
ensemble	NPT	NPT
temp	300 K	300 K
pressure	1 atm	1 atm
avg volume	26.233 nm^3	26.239 nm^3
avg NAD energy	−1101 kJ/mol	−1094 kJ/mol
avg solvent energy	−35101 kJ/mol	−35096 kJ/mol
avg NAD−solvent energy	−1274 kJ/mol	−1295 kJ/mol
avg k-space energy	113 kJ/mol	113 kJ/mol

Recently, the crystal structure of flavin reductase P (FRP) from *Vibrio harveyi* with the inhibitor NAD^+ bound was determined at 2.08-Å resolution.[35] NAD^+ adopts a novel folded conformation in which the nicotinamide and adenine rings stack in parallel. The distance between the centroids of the nicotinamide ring and the 5-membered part of the adenine ring system is 0.36 nm, thus it is the most compact conformation of NAD^+ ever revealed by X-ray crystallography. Given the compact conformation and parallel ring stacking of the bound NAD^+, there is speculation that the reductase structure offers a glimpse of the solution conformation of NAD^+.

The present calculations were performed, in part, to address the question of whether the NAD^+ conformation observed in the flavin reductase structure is stable in solution, which is relevant for understanding the catalytic mechanism of that enzyme. More generally, the simulations provide detailed information about the solution structure and conformational flexibility of NAD^+ that is complementary to the existing experimental data. This information is important for understanding how enzymes recognize, unfold, and bind NAD^+.

Methods

Two classical molecular dynamics simulations of NAD^+ (Figure 1) in explicit water were performed. Explicit solvent was used to provide the most accurate description of solvent effects.[36,37] The setup and results of the simulations are summarized in Tables 1 and 2. Atom-naming conventions are indicated in Figure 1. Dihedral-angle definitions are shown in Figure 1 and listed in Table 2.

(21) Weber, G. *Nature (London)* **1957**, *180*, 1409−10.
(22) Velick, S. F. *J. Biol. Chem.* **1958**, *233*, 1455−67.
(23) Miles, D. W.; Urry, D. W. *J. Biol. Chem.* **1968**, *243*, 4181−88.
(24) Zens, A. P.; Bryson, T. A.; Dunlap, R. B.; Fisher, R. R.; Ellis, P. D. *J. Am. Chem. Soc.* **1976**, *98*, 7559−64.
(25) Oppenheimer, N. J.; Arnold, L. J.; Kaplan, N. O. *Proc. Natl. Acad. Sci. U.S.A.* **1971**, *68*, 3200−5.
(26) Jardetzky, O.; Wade-Jardetzky, N. G. *J. Biol. Chem.* **1966**, *241*, 85−91.
(27) Sarma, R. H.; Ross, V.; Kaplan, N. O. *J. Am. Chem. Soc.* **1968**, *7*, 3052−62.
(28) Meyer, W. L.; Mahler, H. R.; Baker, R. H., Jr. *Biochim. Biophys. Acta* **1962**, *64*, 353−8.
(29) McDonald, G.; Brown, B.; Hollis, D.; Walter, C. *Biochemistry* **1972**, *11*, 1920−30.
(30) Catterall, W. A.; Hollis, D. P.; Walter, C. F. *Biochemistry* **1969**, *8*, 4032−6.
(31) Ellis, P. D.; Fisher, R. R.; Dunlap, R. B.; Zens, A. P.; Bryson, T. A.; Williams, T. J. *J. Biol. Chem.* **1973**, *248*, 7677−81.
(32) Zens, A. P.; Williams, T. J.; Wisowaty, J. C.; Fisher, R. R.; Dunlap, R. B.; Bryson, T. A.; Ellis, P. D. *J. Am. Chem. Soc.* **1975**, *97*, 2850−7.
(33) Riddle, R. M.; Williams, T. J.; Bryson, T. A.; Dunlap, R. B.; Fisher, R. R.; Ellis, P. D. *J. Am. Chem. Soc.* **1976**, *98*, 4286−90.
(34) Jacobus, J. *Biochemistry* **1971**, *10*, 161−4.
(35) Tanner, J. J.; Tu, S.-C.; Barbour, L. J.; Barnes, C. L.; Krause, K. L. *Protein Sci.* **1999**, in press.
(36) Cheatham, T. E., III; Brooks, B. R. *Theor. Chem. Acc.* **1998**, *99*, 279−288.
(37) Smith, P. E.; Pettitt, B. M. *J. Phys. Chem.* **1994**, *98*, 9700−9711.

Table 2. Initial and Final NAD$^+$ Conformations

degree of freedom	definition	FRP structure	$t = 0$ of MD 1	$t = 0$ of MD 2	final[a]
inter-ring distance (nm)	based on centroids of ring systems	0.39	0.38	1.4	0.52
inter-ring angle (deg)	planes defined by C2N, C3N, C5N and C2A, C5A, C8A	14	8	55	148
ζ_N	PA−O3P−PN−O5′N	−94	−105	169	172
α_N	O3P−PN−O5′N−C5′N	149	161	169	67
β_N	PN−O5′N−C5′N−C4′N	180	−176	171	−135
γ_N	O5′N−C5′N−C4′N−C3′N	−140	−149	−167	−69
χ_N	O4′N−C1′N−N1−C2	−140	−137	−146	−106
ω_N	C2N−C3N−C7N−O7N	−173	180	169	free rot.
$\nu_{0,N}$	C4′N−O4′N−C1′N−C2′N	−1	6	−4	−31
$\nu_{1,N}$	O4′N−C1′N−C2′N−C3′N	25	18	32	48
$\nu_{2,N}$	C1′N−C2′N−C3′N−C4′N	−38	−33	−45	−35
$\nu_{3,N}$	C2′N−C3′N−C4′N−O4′N	39	38	46	18
$\nu_{4,N}$	C3′N−CN−C1′N	−24	−28	−26	9
P_N[b]	pseudorotation phase angle	197	208	195	149
ζ_A	PN−O3P−PA-O5′A	90	103	−169	172
α_A	O3P−PA−O5′A−C5′A	−79	−87	−170	−66
β_A	PA−O5A−5′A−C5′A	−85	−90	−92	145
γ_A	O5′A−C5′A−C4′A−C3′A	−77	−68	−68	−56
χ_A	O4′A−C1′A−N9−C4	63	69	71	66
$\nu_{0,A}$	C4′A−O4′A−C1′A−C2′A	−12	−14	−24	−23
$\nu_{1,A}$	O4′A−C1′A−C2′A−C3′A	27	22	33	38
$\nu_{2,A}$	Ci′A−C2′A−C3′A−C4′A	−31	−20	−29	−36
$\nu_{3,A}$	C2′A−C3′A−C4′A−O4′A	24	13	16	25
$\nu_{4,A}$	C3′A−C4′A−O4′A−C1′A	−8	1	4	−1
P_A[b]	pseudorotation phase angle	176	159	153	163

[a] Average over the final 2.5 ns of simulation 1. [b] Describes sugar pucker, tan $P = (\nu_4 + \nu_1 - \nu_3 - \nu_0)/\{2\nu_2(\sin 36° + \sin 72°)\}$; if $\nu_2 < 0$ then $P = P + 180°$.

The two simulations differed only in the initial solute conformation and the simulation time. The initial conformation of NAD$^+$ for simulation 1 was the folded NAD$^+$ obtained from the FRP/NAD$^+$ crystal structure. This system was followed for 5.1 ns, including 0.1 ns of equilibration. Simulation 2 was initiated from an extended model of NAD$^+$ obtained by adjusting the ζ_N, ζ_A, and α_A dihedral angles of the FRP/NAD$^+$ crystal structure to −180°. A total of 2.6 ns of dynamics was generated, including 0.1 ns of equilibration.

The force field of Pavelites et al.[38] was used for NAD$^+$, together with the TIP3P water model.[39] NAD$^+$ was solvated by placing it in a pre-equilibrated cubic box of water molecules and removing waters which were within 0.2 nm from any non-hydrogen atom of the solute. Both systems contained one NAD$^+$ and 867 water molecules in a box of length 3.0 nm. Each system was minimized with 100 steps of steepest descent (see $t = 0$ columns of Table 2) and equilibrated for 0.1 ns. For the first 0.05 ns of the equilibration the masses of the solute atoms were increased by a factor of ten to ensure preferential equilibration of the solvent molecules, and velocities were reassigned every 1 ps to avoid local heating artifacts. None of the energy terms displayed a discernible drift with time after the initial equilibration period.

Simulations were performed in the NPT ensemble at 300 K and 1 atm using the weak coupling technique to modulate the temperature and pressure[40] with relaxation times of 0.1 and 0.5 ps, respectively. SHAKE[41] was used to constrain all bonds with a relative tolerance of 10^{-4}, allowing a 2-fs time step. Configurations and energies were saved every 0.1 ps for analysis.

Electrostatic interactions were calculated using the Ewald technique[42] using a convergence parameter of 2.5 nm^{-1} and a real space cutoff of 1.2 nm and including all lattice vectors with $n^2 \leq 64$. Ewald artifacts are expected to be negligible due to the high relative permittivity of water.[43,44] In order to avoid possible problems associated with simulating a charged Ewald system,[45] the solute was neutralized by the addition of a unit positive charge, equally partitioned over all 70 NAD$^+$ atoms. Similar approaches have been used previously.[46,47] Charge neutralization required only a small adjustment of +0.0143e to each atomic charge. To test the validity of this approach, the 5.1-ns simulation described above was continued for a further 1.0 ns using a different charge neutralization scheme in which +0.25e was added to the partial charges of O1PN, O2PN, O1PA, and O2PA. No significant changes from the previous simulation were observed, suggesting that the results described below were not artifacts of the charge neutralization method.

Analysis of interaction energies and radial distribution functions (rdfs) was performed on a group basis. Groups were defined by the sets of atoms that are isolated after breaking the following bonds: N1−C1′N, C5′N−O5′N, O5′A−C5′A, C1′A−N9. The five resulting groups were denoted as N (nicotinamide), R_N, (nicotinamide ribose), P (pyrophosphate), R_A (adenine ribose), and A (adenine). The center of mass was used to define the position of each group. The interaction energies between different groups, and between different groups and the solvent, were obtained using the van der Waals energy and the standard Coulomb potential (not the Ewald potential). The latter ap-

(38) Pavelites, J. J.; Gao, J.; Bash, P. A.; Mackerell, A. D., Jr. *J. Comput. Chem.* **1997**, *18*, 221−239.
(39) Jorgensen, W. L.; Chandrasekhar, J.; Madura, J. D.; Impey, R. W.; Klein, M. L. *J. Chem. Phys.* **1983**, *79*, 926−35.
(40) van Gunsteren, W. F.; Berendsen, H. J. C. *Angew. Chem., Int. Ed. Engl.* **1990**, *29*, 992−1023.
(41) Ryckaert, J. P.; Ciccotti, G.; Berendsen, H. J. C. *J. Comput. Phys.* **1977**, *23*, 327−41.
(42) de Leeuw, S. W.; Perram, J. W.; Smith, E. R. *Proc. R. Soc. London, Ser. A* **1980**, *373*, 27−56.
(43) Smith, P. E.; Pettitt, B. M. *J. Chem. Phys.* **1996**, *105*, 4289−93.
(44) Huenenberger, P. H.; McCammon, J. A. *J. Chem. Phys.* **1999**, *110*, 1856−72.
(45) Bogusz, S.; Cheatham, T. E., III; Brooks, B. R. *J. Chem. Phys.* **1998**, *108*, 7070−84.
(46) Northrup, S. H.; Pear, M. R.; Morgan, J. D.; McCammon, J. A.; Karplus, M. *J. Mol. Biol.* **1981**, *153*, 1087−1109.
(47) van Gunsteren, W. F.; Berendsen, H. J. C. *Groningen Molecular Simulation (GROMOS) Library Manual*; van Gunsteren, W. F., Berendsen, H. J. C., Eds.; Biomos: Groningen, 1987.

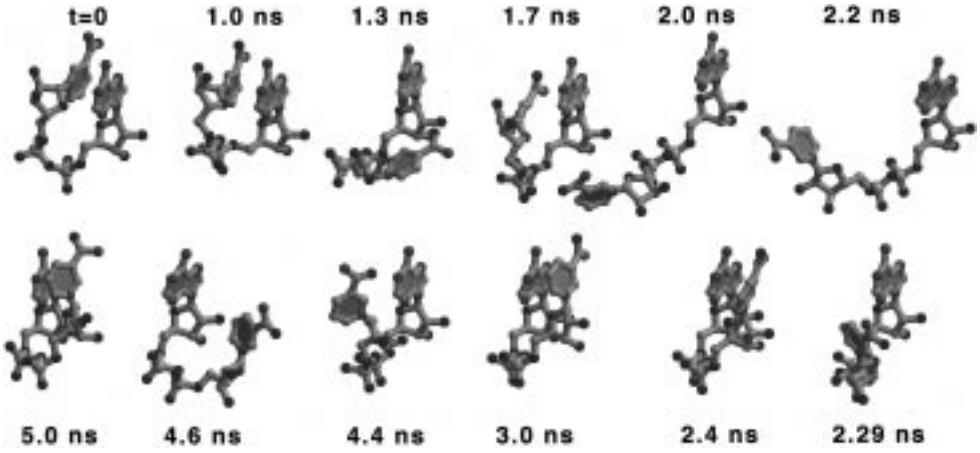

Figure 2. NAD^+ conformations obtained from simulation 1. The structures have been rotated and translated so that the orientation of the adenine and its ribose is constant. Figure prepared with Molscript.[55]

proximation was used to circumvent the problem of deconvoluting the reciprocal space term into atom−atom interactions.[48]

Accessible surface are (ASA) calculations were performed using X-plor[49] with a probe radius of 0.14 nm and a grid accuracy of 0.025. Inter-ring distances were based on the centroids of the six-membered nicotinamide ring (N1, C2, C3, C4, C5, C6) and the nine-membered adenine ring system (N1, C2, N3, C4, C5, C6, N7, C8, N9). The inter-ring angle was defined as the angle between the plane containing the nicotinamide C2, C3, and C5 atoms and the plane containing the adenine C2, C5, and C8 atoms. Coordination numbers were determined by integration of the appropriate radial distribution functions.[48] Statistical errors were estimated by calculating the standard deviation between three or four block subaverages.

Results

Dynamics of NAD^+ in Solution. Simulation 1 was initiated from the highly compact NAD^+ conformation observed in the FRP/NAD^+ crystal structure. Here, the nicotinamide ring is stacked in parallel above the 5-membered part of the adenine at a distance of 0.36 nm (Figure 2, $t = 0$). The nicotinamide and adenine ribose rings adopt the $C_{3'}$-exo and $C_{2'}$-endo conformations, respectively. The χ angles indicate anti and syn conformations for the nicotinamide and adenine, respectively.

The progress of simulation 1 is shown in terms of structures in Figure 2 and calculated quantities in Figure 3. The time history can be divided into three main regions, $t = 0-1.8$, $t = 1.8-2.5$, and $t = 2.5-5.1$ ns. The first time slice was dominated by conformations similar to that of the FRP crystal structure. The initial NAD^+ conformation persisted for the first 1 ns of the simulation, followed by an unfolding transition to a moderately extended conformation at 1.3 ns and a return to the initial conformation. The second time slice was characterized by complete unfolding of the molecule into highly extended conformations ($t = 2.0$, 2.2 ns), followed by refolding into a compact conformation that was different from the initial conformation. During the final 2.6 ns of the simulation, the new folded conformation persisted, along with other moderately extended conformations resulting from unfolding events at $t = 4.4$ and 4.6 ns. The rmsd plot (Figure 3) clearly illustrates that the final form of NAD^+ obtained from the simulation deviated by more than 0.6 nm from the initial folded form.

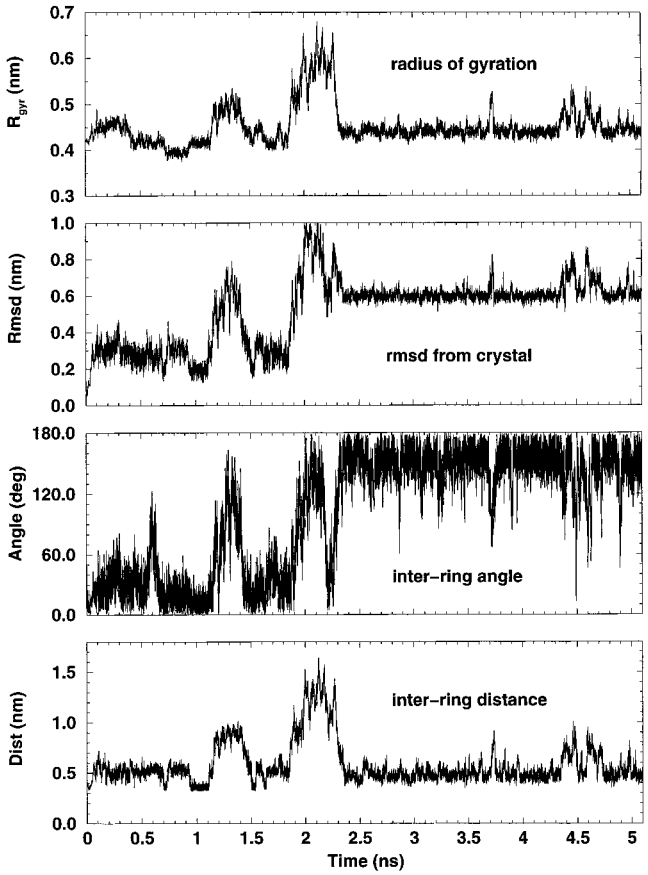

Figure 3. Time histories of the radius of gyration, rmsd from the initial conformation, inter-ring angle, and inter-ring distance for simulation 1.

Time histories of several dihedral angle degrees of freedom characterizing the dynamics and conformation of NAD^+ are displayed in Figure 4. The dihedral angles that remained in a single conformation for the majority of the simulation (ζ_N, ζ_A, χ_N, and χ_A) or that displayed facile interconversion between rotational states (ω_N, ribose hydroxyl group dihedrals) are not shown. Several dihedral-angle transitions were observed for the α and γ dihedrals which correlated with the major changes in the R_g, rmsd, angle, and distance time histories shown in Figure 3.

The major transition between the initial folded form and the final folded form (1.8−2.5 ns) was most strongly correlated with sharp transitions in α_N and γ_N and small changes in β_A.

(48) Allen, M. P.; Tildesley, D. J. *Computer Simulation of Liquids*; Oxford University Press: Oxford, 1987.

(49) Brünger, A. T. *X-PLOR*, version 3.1; A system for x-ray crystallography and NMR; Yale University Press: New Haven, 1992.

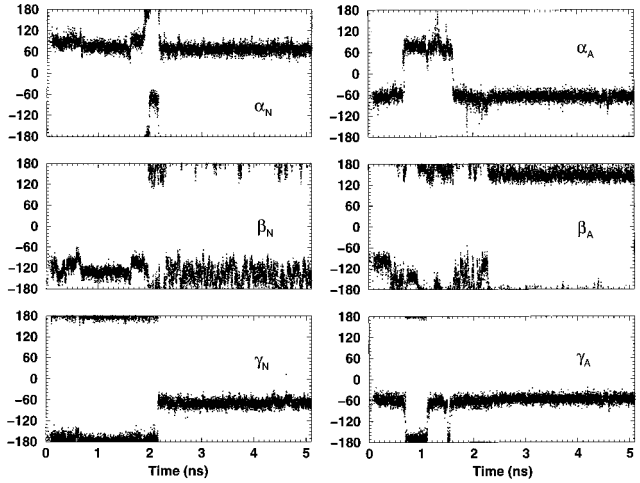

Figure 4. Time histories of selected dihedral angles from simulation 1.

No dihedral transitions were observed after 2.5 ns, indicating that a single relatively stable folded structure had been generated. However, the data in Figure 3 clearly show that the final folded structure fluctuated significantly to the extent that the aromatic rings were no longer stacked and inter-ring distances of 1.0 nm were observed. Hence, even the folded structure was flexible enough to periodically expose and fully solvate both aromatic rings.

As a test of the reproducibility of the results, a second simulation was started from an extended NAD$^+$ model (see Table 2). The progress of this simulation is shown in Figure 5. The unfolded model of NAD$^+$ converged within 0.6 ns to a folded conformation that was very similar to that obtained in simulation 1. The final conformations from the two simulations possessed an all-atom rmsd of only 0.1 nm and nearly identical R_g and inter-ring distances. The average structures calculated from $t = 2.5-5.1$ ns of simulation 1 and $t = 0.7-2.6$ ns of simulation 2 superimpose with an rmsd of 0.027 nm. Hence, two different simulations of NAD$^+$ in solution, starting from different initial conformations, produced identical folded conformations. The degree of reproducibility observed here suggests that the simulations displayed a reasonable degree of conformational sampling for this system. This fact, coupled with the quality of the force field, also suggests that the present simulation can describe the structure and dynamics of NAD$^+$ in solution with reasonable precision and accuracy.

Structure of NAD$^+$ in Solution. Since the two simulations converged to a common conformation, the following discussion will focus on the results of simulation 1. The average structural parameters obtained from the final 2.5 ns of simulation 1 are presented in Table 2. The average inter-ring distance was 0.52 nm with an rms fluctuation of 0.097 nm. The average angle between the two ring systems was 148° with an rms fluctuation of 19°. Both sugar puckers were in the $C_{2'}$-endo orientation. The nicotinamide ring adopted an anti conformation, while the adenine ring was syn to the ribose. The pyrophosphate linkage remained rigid after the equilibration period with both ζ dihedrals in the trans arrangement.

The structure obtained at $t = 5$ ns was typical of the average folded conformation, with an inter-ring distance of 0.45 nm and inter-ring angle of 140°. This structure is compared with the starting structure and with a model based on molecular mechanics calculations[50] in Figure 6. The molecular mechanics model is the lowest energy conformation obtained from minimization in vacuum. The three models have several significant differences. First, the crystal structure model (Figure 6a) and the molecular mechanics model (Figure 6c) display almost perfectly parallel ring stacking with inter-ring distances of less than 0.4 nm, which implies substantial π-stacking interactions. The solvated structure (Figure 6b), however,

(50) Thornton, J. M.; Bayley, P. M. *Biopolymers* **1977**, *16*, 1971−86.

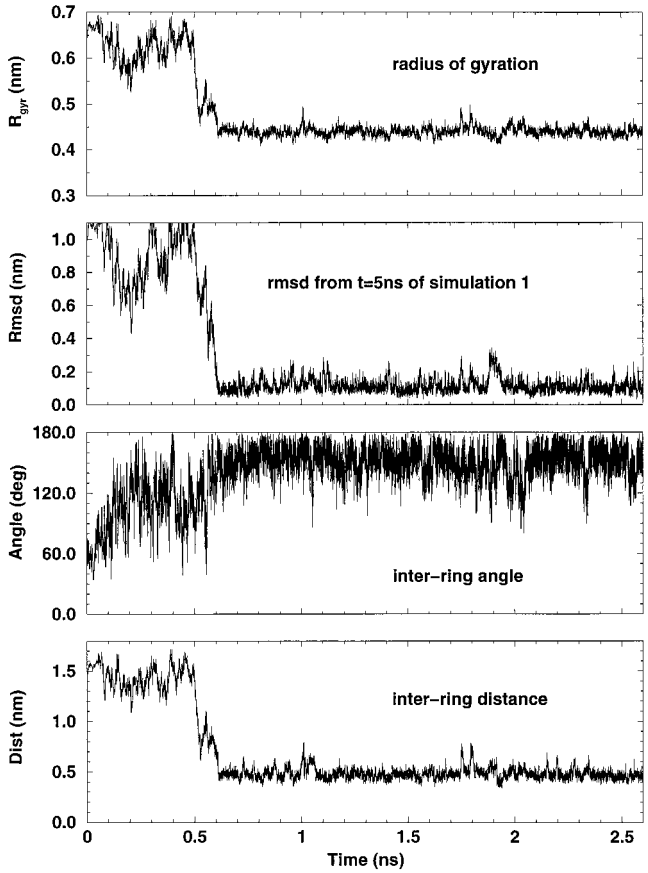

Figure 5. Time histories of the radius of gyration, rmsd from the $t = 5$ ns conformation of simulation 1, inter-ring angle, and inter-ring distance for simulation 2.

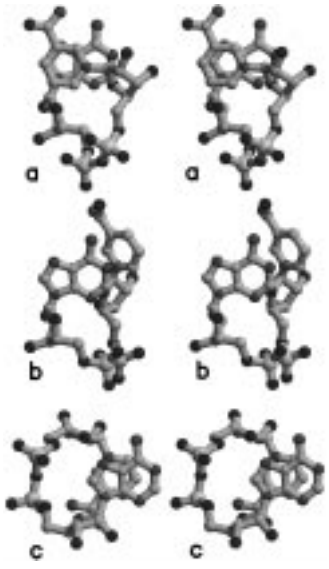

Figure 6. Stereo views of NAD$^+$ structures; the FRP/NAD$^+$ crystal structure (a), the $t = 5$ ns configuration of simulation 1 (b), and the model of Thornton and Bayley (c). The structures have been rotated and translated so that the orientation of the adenine and its ribose is constant. Figure prepared with Molscript.[55]

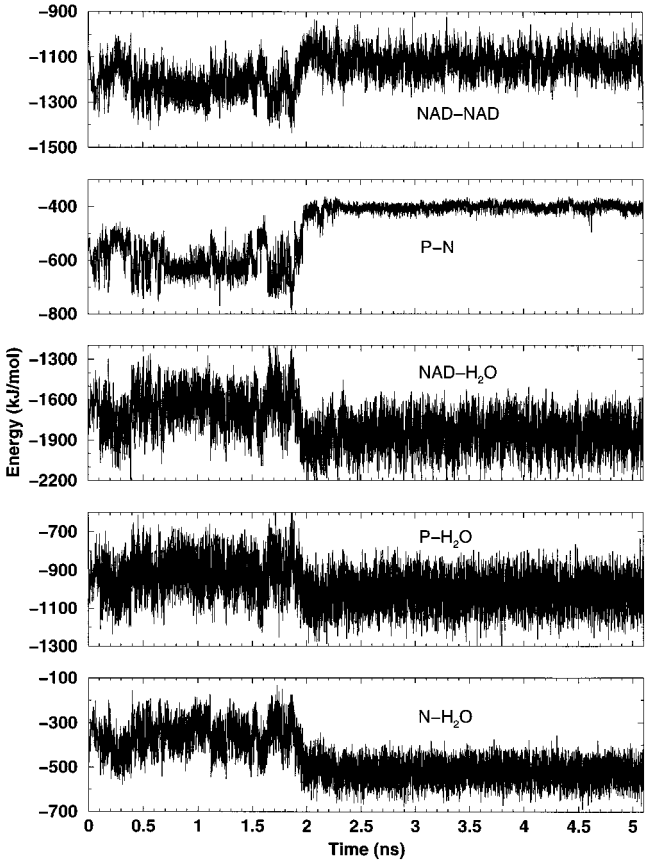

Figure 7. Time histories of various interaction energies from simulation 1.

exhibits less inter-ring interaction. Second, the relative orientations of the nicotinamide and adenine rings are different. Using the adenine orientation in Figure 6 as a reference, both the solvated model and the molecular mechanics models show the adenine stacked on top of the nicotinamide, whereas the crystal structure shows the opposite arrangement. Third, the glycosyl bond vectors are perpendicular in the FRP crystal structure, parallel in the solvated model, and anti-parallel in the molecular mechanics model. Fourth, the molecular mechanics model has both rings in anti conformations, whereas the crystal structure and solvated models show anti conformations for the nicotinamide and syn conformations for the adenine. Fifth, both the FRP and molecular dynamics models have the nicotinamide B side facing the adenine, while the molecular mechanics model has the A side packed against the adenine.

NAD^+−Water Interactions. The pyrophosphate group of NAD^+ was found to be rigid with both ζ dihedrals in the trans arrangement. This conformation was adopted early in the simulation and persisted until the end. The rigidity of the pyrophosphate group was unexpected as the intrinsic barriers to rotation around these dihedrals are low (approximately 1 kJ/mol).[38] The difference appears to relate to a strong explicit solvation effect.[54] This suggests that the pyrophosphate arrangement displayed in the molecular mechanics model (Figure 6c, $\zeta_A = -53°$), produced using a simple dielectric model, would be unstable in solution.

To understand the folding/unfolding characteristics of NAD^+ in solution, the energetics and solvation properties of the different conformations of NAD^+ were investigated. A series of energy time histories is displayed in Figure 7. This data clearly indicated a significant change in several of the intra- and intermolecular energy terms between 1.8 and 2.1 ns,

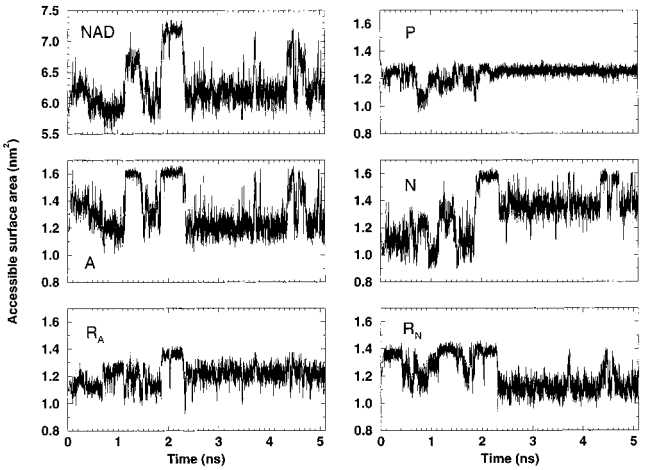

Figure 8. Time histories of the accessible surface areas of NAD^+ and its constituent groups from simulation 1.

corresponding to the observed dihedral transition around γ_N. Other dihedral transitions did not significantly affect the nonbonded interactions of the system.

Considering only the two major conformations obtained during the simulation, one before 1.8 ns and the other after 2.5 ns, it is clear that after the transition between these two forms the NAD^+−NAD^+ interactions were weakened at the expense of more favorable NAD^+−H_2O interactions (Figure 7). The latter correlated with improved pyrophosphate and nicotinamide solvation energies. Hence, changes in solvation appeared to be the major cause, or stabilization effect, of the conformational change. This is to be expected as the nicotinamide and pyrophosphate carry formal charges. No significant changes were observed for the nicotinamide to adenine interaction energy during any of the folding/unfolding transitions, suggesting that π-stacking effects, as described by the current classical force field, were not responsible for the conformational properties of NAD^+ in solution.

The accessible surface are (ASA) of NAD^+, and of specific groups within the molecule, is displayed in Figure 8. The ASA of NAD^+ increased on going from the FRP conformation to the final folded form. The largest increase in ASA was observed for the nicotinamide ring. In contrast, the nicotinamide ribose became more buried after the transition. Large fluctuations in the total ASA were seen during $t = 2.5-5.1$ ns, which confirmed the observation that water penetration between the bases occurred even while NAD^+ retained an overall folded conformation.

Radial distribution functions (rdfs) between NAD^+ and the solvent are shown in Figure 9. These rdfs were calculated for the two major folded conformations of simulation 1 and for an ensemble of unfolded structures obtained from the first 0.5 ns of simulation 2. As expected, the unfolded form displayed the highest degree of solvation of the three NAD^+ conformations due to the larger accessible surface area. None of the groups possessed particularly strong first solvation shells, with the possible exception of the pyrophosphate group. This is probably a consequence of the diffuse nature of the formal charges on the pyrophosphate and nicotinamide groups. There were some small, but significant, differences between the solvation characteristics of the two folded forms of NAD^+ as described by the rdfs; however, the solvation effects were more apparent when one examined the changes in the corresponding water coordination numbers.

Figure 10 shows the difference in coordination number (average number of water molecules found within a distance r)

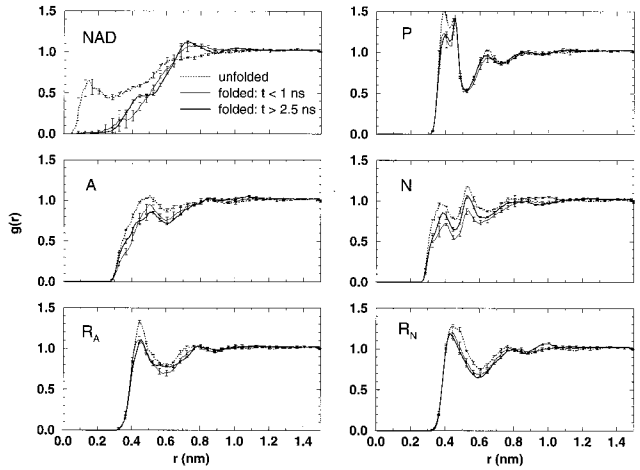

Figure 9. Radial distribution functions between NAD$^+$ groups and water as a function of conformation. The dashed curve represents an unfolded form (0−0.5 ns of simulation 2) and the solid curves represent the two major folded forms observed in simulation 1. Error bars represent one standard deviation.

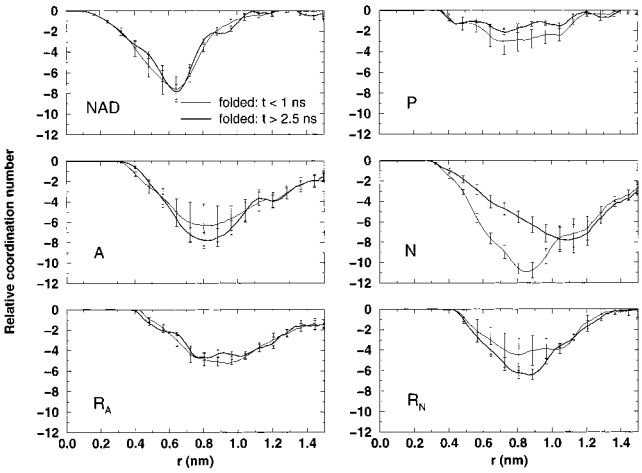

Figure 10. Difference in coordination number between the two folded conformations of simulation 1 and an unfolded conformation from simulation 2 for each of the groups of NAD$^+$. The *y* axis represents the change in solvation (in units of number of water molecules) for the different conformations. Error bars represent one standard deviation.

between folded and unfolded forms of NAD$^+$. In these plots, zero corresponds to the coordination number of an extended NAD$^+$ molecule, while increasingly negative values indicate lesser degrees of solvation. All values were negative, illustrating the higher solvation of the unfolded conformation. Differences between folded and unfolded forms were largest for the nicotinamide group, with the nicotinamide being more heavily solvated at smaller distances in the final folded form than in the initial FRP form. The nicotinamide solvation changes mirrored the changes in interaction energies observed in Figure 7 and were particularly significant because of the charged nature of the group. In contrast, the changes observed for the NAD$^+$/H_2O and P/H_2O interaction energies are not apparent in the coordination difference plots. In these two cases one has to conclude that the solvation energy changes probably resulted from changes in the orientation preferences of water molecules surrounding these groups. Hence, the major difference between the two folded conformations of NAD$^+$ observed in simulation 1 appeared to be the higher solvation of the nicotinamide group in the final folded form. The different solvation characteristics observed here were unusual in that they appeared to be dominated by changes in the long-range solvent distribution (0.6−1.0 nm), probably related to long-range electrostatic effects. These results underscore the importance of treating long-range interactions carefully.[51,52]

Discussion

Several experiments suggest a folded NAD$^+$ exists in solution, including circular dichroism, fluorescence spectroscopy, NMR, and X-ray crystallography experiments. While an atomic model for the solution structure cannot be easily derived from these experiments, a few major structural parameters have been postulated.

NMR chemical shift experiments suggest a model in which the aromatic rings stack in parallel at a distance of less than 0.39 nm with the B side of the nicotinamide folded against the adenine[25,27] and 15−40% of the dinucleotide present in a folded conformation.[26,29] Likewise, Miles and Urry[23] used circular dichroism and absorption spectroscopy to propose a parallel-stacked structure with the nicotinamide B side folded against the adenine.

Saenger's Li$^+$-NAD$^+$ crystal structure shows an extended NAD$^+$ similar to those bound to enzymes; however, the crystal packing in that structure results in intermolecular parallel ring stacking in which the two rings are 0.31 nm apart, the glycosyl bond vectors are antiparallel, and the A side of the nicotinamide is packed against the adenine.[19,20] Reddy et al. propose that these intermolecular interactions might be important intramolecular interactions in solution.[19] Thornton and Bayley's calculations agree with this proposal.[50] Their lowest energy conformation, which was obtained from vacuum molecular mechanics calculations, shows the two rings stacked within van der Waals contact with antiparallel glycosyl band vectors and the A side of the nicotinamide folded against the adenine.

The crystal structure of flavin reductase P with NAD$^+$ bound[35] in the active site is another piece of evidence that relates to the folded form of NAD$^+$. The dinucleotide, somewhat surprisingly, adopts a compact folded conformation in which the rings stack in a nearly parallel fashion with a distance of 0.36 nm between the nicotinamide ring and the 5-membered ring of the adenine. This conformation displays perpendicular glycosyl bond vector with the B side of the nicotinamide folded against the adenine. The question of how this conformation relates to the solution form of NAD$^+$ is complicated by the fact that the NAD$^+$ appears in the active site of an enzyme and there are crystal contacts that might influence the conformation.

A different picture of the solution form of NAD$^+$ emerges from the NMR proton spin-lattice relaxation time studies of Zens et al.[24] They conclude that the two rings do not approach each other closer than 0.45 nm for periods comparable to the reorientational time of NAD$^+$ (0.26 ns). These data imply a less compact conformation than has been proposed by others, and they suggest that stacking interactions are not important for stabilizing the folded conformation of NAD$^+$.

Thus, while there is much experimental evidence suggestive of a folded NAD$^+$ in a solution, there is disagreement over the details of the conformation, particularly concerning the extent and nature of the interaction between the aromatic rings. Moreover, Jacobus disputed the interpretation of the chemical shift data and asserted that it could not be used to define

(51) Smith, P. E.; Pettitt, B. M. *J. Chem. Phys.* **1991**, *95*, 8430−41.
(52) Smith, P. E.; van Gunsteren, W. F. Methods for the Evaluation of Long Range Electrostatic Forces in Computer Simulations of Molecular Systems. In *Computer Simulation of Biomolecular Systems: Theoretical and Experimental Applications, Vol. 2*; van Gunsteren, W. F., Weiner, P. K., Wilkinson, A. J., Eds.; ESCOM: Leiden, 1993; pp 182−212.

unambiguously the molecular geometry.[34] In addition, it has been noted that the nature of the counter ion in the NMR experiments was not clear, and on the basis of the strong Li^+ pyrophosphate interaction in the Li^+-NAD^+ crystal structure, the counter ion could prove important in determining the folded conformation.[19]

The molecular dynamics calculations presented here were performed to gain insight into the nature of the solution structure of NAD^+ by providing data complementary to the existing experimental data. The two simulations were started from different conformations, but they resulted in a common conformation that is highlighted by an average inter-ring distance of 0.52 nm, an average inter-ring angle of 148°, nearly parallel glycosyl bond vectors, and the nicotinamide B side facing the adenine.

The final molecular dynamics conformation seems to be preferred over the initial, highly compact conformation of simulation 1 because of improved solvation of the charged nicotinamide ring. On the other hand, the final molecular dynamics conformation is preferred over the initial extended conformation of simulation 2 because of its higher buried surface area and lower surface to volume ratio, which are two important factors in the folding of larger biomolecules, such as proteins. Thus, the conformation obtained in the simulations appears to be a compromise between the burial of molecular surface area and solvation of the charged nicotinamide ring.

The inter-ring distance and nonparallel arrangement of the aromatic rings in the major molecular dynamics conformation are consistent with the "less restrictive" model suggested by Ellis.[24,32,33] The interaction of the nicotinamide B side with adenine is in agreement with several experimental studies.[23,25,27] The molecular dynamics model obtained here is highly folded in comparison with typical enzyme-bound NAD^+, but less compact than models based on chemical shift data,[23,25−27] inferred from crystal packing,[19] or predicted from molecular mechanics calculations.[50]

The fraction of time spent in a folded conformation estimated from the simulation is higher than that deduced from NMR data;[26−29] however, the definition of "folded" is open to interpretation, and the accuracy of these experimental values could be questioned considering the disagreement concerning the interpretation of the NMR data[34] and the influence of counter ions.[19] One important consideration is that the present simulations may not have sampled all the possible conformations of NAD^+ in solution, and this could explain some of the discrepancy in the calculated ratio of folded to unfolded forms. Of particular note is the lack of χ_N transitions.[32,53] Additionally, the simulations did not consider the effects of salt, and in particular, cation binding to the pyrophosphate. Furthermore, although Ewald artifacts are not expected in this system,[43,44] they may slightly favor a more folded form of NAD^+ because of increased attraction between oppositely charge groups.[44] Nonetheless, the reproducibility of the simulation results, together with the apparent stability of the final folded form, suggest that the folded conformation of NAD^+ observed here is plausible and requires further theoretical and experimental investigation.

Finally, the simulations suggest that the NAD^+ conformation observed in the FRP/NAD^+ crystal structure is not stable in solution. Therefore, inhibition of the enzyme by NAD^+ involves a novel conformation that is neither the folded solution form nor a previously observed extended conformation. The FRP/NAD^+ crystal structure shows, for the first time, that it is possible for a protein surface to recognize and bind a highly compact, folded NAD^+;[35] thus, it might be possible to engineer a protein binding site that recognizes the folded, solution form of NAD^+. The present calculations, and similar future ones, will provide essential information for this protein design effort.

Conclusion

Molecular dynamics simulations have been used to study the conformational properties of NAD^+ in solution. The reproducibility of the calculations was confirmed by performing two simulations with different initial starting configurations. The major folded forms of NAD^+ obtained from the two simulations were identical. This observation, coupled with the use of high-quality force field specific for NAD^+, suggests that the simulations should provide accurate information on this molecule. The major folded form of NAD^+ observed during the simulations is consistent with NMR relaxation data, but it is less compact than folded conformations proposed previously. In particular, the aromatic rings do not adopt a perfect parallel stacking arrangement, and solvent exposure of the two rings occurred even while the molecule remained in an overall folded conformation. The preferred conformation in solution appears to be a compromise between burial of molecular surface area and exposure of the nicotinamide group to the solvent. Further work is required to determine the full range of possible folded and unfolded forms of NAD^+ in solution.

Acknowledgment. The authors would like to thank Alex Mackerell, Jr. for making the NAD force field parameters available. This project was partially supported by the Kansas Agricultural Experimental Station (Contribution 99-465-J) (P.E.S.) and a Big 12 faculty fellowship award (J.J.T.).

JA991624B

(53) Egan, W.; Forsen, S.; Jacobus, J. *Biochemistry* **1975**, *14*, 735−42.

(54) The rigidity of the pyrophosphate group appears to be sensitive to the solvent model. Using the same NAD^+ force field, a stochastic dynamics simulation at 300 K employing a dielectric constant of 80 approximation resulted in essentially free rotation (barriers less than 5 kJ/mol) around both ζ dihedrals.

(55) Kraulis, P. J. *J. Appl. Crystallogr.* **1991**, *24*, 946−950.